



# HHS Public Access

Author manuscript

*Mol Cancer Res.* Author manuscript; available in PMC 2017 December 01.

Published in final edited form as:

*Mol Cancer Res.* 2016 December ; 14(12): 1266–1276. doi:10.1158/1541-7786.MCR-16-0233.

## MUC1-C Represses the Crumbs Complex Polarity Factor CRB3 and Downregulates the Hippo Pathway

Maroof Alam<sup>1</sup>, Audrey Bouillez<sup>1</sup>, Ashujit Tagde<sup>1</sup>, Rehan Ahmad<sup>1,+</sup>, Hasan Rajabi<sup>1</sup>, Takahiro Maeda<sup>1</sup>, Masayuki Hiraki<sup>1</sup>, Yozo Suzuki<sup>1,\*</sup>, and Donald Kufe<sup>1</sup>

<sup>1</sup>Dana-Farber Cancer Institute, Harvard Medical School, Boston, MA

### Abstract

Apical-basal polarity and epithelial integrity are maintained in part by the Crumbs (CRB) complex. The C-terminal subunit of MUC1 (MUC1-C) is a transmembrane protein that is expressed at the apical border of normal epithelial cells and aberrantly at high levels over the entire surface of their transformed counterparts. However, it is not known if MUC1-C contributes to this loss of polarity that is characteristic of carcinoma cells. Here it is demonstrated that MUC1-C downregulates expression of the Crumbs complex CRB3 protein in triple-negative breast cancer (TNBC) cells. MUC1-C associates with ZEB1 on the CRB3 promoter and represses CRB3 transcription. Notably, CRB3 activates the core kinase cassette of the Hippo pathway, which includes LATS1 and LATS2. In this context, targeting MUC1-C was associated with increased phosphorylation of LATS1, consistent with activation of the Hippo pathway, which is critical for regulating cell contact, tissue repair, proliferation and apoptosis. Also shown is that MUC1-C-mediated suppression of CRB3 and the Hippo pathway is associated with dephosphorylation and activation of the oncogenic YAP protein. In turn, MUC1-C interacts with YAP, promotes formation of YAP/ $\beta$ -catenin complexes and induces the WNT target gene MYC. These data support a previously unrecognized model in which targeting MUC1-C in TNBC cells (i) induces CRB3 expression, (ii) activates the CRB3-driven Hippo pathway, (iii) inactivates YAP, and thereby (iv) suppresses YAP/ $\beta$ -catenin-mediated induction of MYC expression.

**Implications**—These findings demonstrate a previously unrecognized role for the MUC1-C oncoprotein in the regulation of polarity and the Hippo pathway in breast cancer.

### Keywords

MUC1; CRB3; Hippo; YAP; triple-negative breast cancer; MYC

### Introduction

Epithelia are comprised of a laterally connected layer of cells with apical-basal polarity. The epithelial stress response is associated with loss of apical-basal cell polarity and disruption

<sup>†</sup>Present address: College of Medicine, King Saud University, Riyadh, Saudi Arabia

<sup>\*</sup>Present address: Department of Gastroenterological Surgery, Osaka Police Hospital, Kitayama-Cho 10-31 Tennoji, Osaka City, Osaka 543-0035, Japan

**Potential Conflict of Interest:** The authors declare competing financial interests: D.K. holds equity in Genus Oncology and is a consultant to the company. The other authors disclosed no potential conflicts of interest.

of cell-cell adhesion (1, 2). Loss of polarity thereby constitutes an early step in the epithelial to mesenchymal transition (EMT), whereby epithelial cells acquire invasive and migratory properties. Apical-basal polarity is maintained by: (i) the Scribble complex (Scrib, Dlg, Lgl) responsible for establishing the basolateral membrane domain, (ii) the PAR complex (Cdc42, PAR3/ASIP, PAR6, atypical protein kinase C) at the apical-lateral junctions between cells, and (iii) the Crumbs complex (Crb, PALS, PATJ, Lin7), which defines the apical membrane (2). Cell polarity is thus maintained as a result of mutual interactions among the PAR, CRB and SCRIB complexes (3). Three orthologs of the *Drosophila* Crb protein are expressed in human tissues, named CRB1, CRB2, and CRB3, of which CRB3 is predominantly found in epithelial cells and suppresses epithelial tumor progression (2). Additionally, CRB3 functions as a tumor suppressor by activating the Hippo signaling network (mammalian orthologs SAV1, MST1/2 and LATS1/2) (4, 5). The Hippo pathway has been linked to cancer stem-like cells, invasion, DNA repair and therapeutic resistance (4, 6–8). Moreover, the Hippo pathway intersects with the canonical WNT/ $\beta$ -catenin pathway (4, 9). The major downstream effectors of the Hippo pathway are the transcriptional co-activator with PDZ-binding motif (TAZ) and the Yes-associated protein (YAP) (10). TAZ activates Dishevelled and represses  $\beta$ -catenin (9); whereas, YAP binds directly to  $\beta$ -catenin (11). CRB3-mediated activation of the Hippo kinase cascade results in the downstream phosphorylation and inactivation of YAP (10, 12). Phosphorylated YAP is retained in the cytoplasm and thereby inhibits the WNT/ $\beta$ -catenin pathway by binding to  $\beta$ -catenin and restricting its translocation to the nucleus (10, 12, 13). However, in response to CRB3 suppression, the Hippo pathway is inactivated, leading to dephosphorylation and activation of YAP (4). In turn, localization of the YAP/ $\beta$ -catenin complex in the nucleus promotes the induction of certain WNT target genes (10, 11, 14, 15).

Mucin 1 (MUC1) is a transmembrane protein that is widely overexpressed in breast and other carcinomas (16). MUC1 undergoes an autocleavage process, resulting in an extracellular N-terminal subunit (MUC1-N) and a transmembrane C-terminal subunit (MUC1-C), which form complexes at the apical membranes of normal epithelial cells (16, 17). With loss of cell polarity, the oncogenic MUC1-C subunit is expressed over the entire cell membrane, and interacts with receptor tyrosine kinases (RTKs), such as EGFR, which are typically positioned at the basal-lateral borders (16, 17). As a consequence of this association with RTKs, MUC1-C upregulates RTK signaling by promoting activation of the downstream PI3K $\rightarrow$ AKT and MEK $\rightarrow$ ERK pathways (16–21). In addition, MUC1-C is imported into the nucleus, where it interacts with transcription factors, such as NF- $\kappa$ B p65 and ZEB1, among others (16, 17, 22, 23). The MUC1-C cytoplasmic domain binds directly to NF- $\kappa$ B p65 and increases occupancy of NF- $\kappa$ B on the promoters of its target genes (22). In this context, MUC1-C/NF- $\kappa$ B p65 complexes activate the *ZEB1* promoter and increase ZEB1 expression (23). Further, MUC1-C associates with ZEB1 to repress the *miR-200c* gene, which encodes a tumor suppressor that reverses EMT (23). MUC1-C also binds directly to  $\beta$ -catenin, stabilizes  $\beta$ -catenin/TCF4 complexes and thereby promotes activation of WNT target genes, such as *CCND1* and *MYC* (24–28).

To our knowledge, there is no available evidence supporting involvement of MUC1-C in the regulation of apical-basal polarity. The present results demonstrate that MUC1-C represses the CRB3, HUGL2 and PATJ polarity factors in TNBC cells, indicating that MUC1-C is of

importance to the loss of cell polarity. Based on the role of CRB3 in activating the Hippo pathway, the present work has focused on the downstream effects of MUC1-C-mediated CRB3 suppression. We show that MUC1-C represses *CRB3* transcription and downregulates the Hippo pathway. In addition, we show that MUC1-C activates YAP and forms a complex with YAP/ $\beta$ -catenin that activates the *MYC* promoter. Our findings thus demonstrate that targeting MUC1-C activates the CRB3→Hippo tumor suppressor cascade.

## Materials and Methods

### Cell culture

Human MDA-MB-231, BT-20 and MCF-7 breast cancer cells were cultured in DMEM (Dulbecco's Modified Eagle's Medium) growth medium containing 10% heat-inactivated fetal bovine serum, 100 units/ml penicillin, 100  $\mu$ g/ml streptomycin and 2 mM L-glutamine. Human BT-549 breast cancer cells were grown in RPMI1640 medium with heat-inactivated fetal bovine serum, antibiotics, L-glutamine and 10  $\mu$ g/ml insulin. Authentication of the cells was confirmed by short tandem repeat (STR) analysis. MDA-MB-231 and BT-549 cells were infected with lentiviral vectors that express a MUC1shRNA (MISSION shRNA TRCN0000122938; Sigma, St Louis, MO) or scrambled control shRNA (CshRNA; Sigma) (29). BT-20 and MCF-7 cells were transfected with a pHR-CMV vector expressing MUC1-C or with an empty vector. Cells were also infected with lentiviral vectors expressing a SNAIL1 shRNA (MISSION shRNA TRCN0000063822; Sigma), a ZEB1 shRNA (MISSION shRNA TRCN0000017565; Sigma) or a scrambled control shRNA vector (CshRNA; Sigma). Cells were also infected with lentivirus vectors expressing a tetracycline-inducible MUC1shRNA (tet-MUC1shRNA), as described (30). MUC1shRNA (MISSION shRNA TRCN0000122938; Sigma) or a control scrambled CshRNA (Sigma) was inserted into the pLKO-tet-puro vector (Addgene, Plasmid #21915). The viral vectors were produced in HEK293T cells as previously described (30, 31). Cells expressing tet-MUC1shRNA or tet-CshRNA were selected for growth in 1–3  $\mu$ g/ml puromycin. Cells were (i) treated with doxycycline (DOX; Sigma), and (ii) transfected with a CRB3 siRNA (sc43698) or a control siRNA (sc37007) (Santa Cruz Biotechnology).

### Immunoprecipitation and immunoblot analysis

Whole cell lysates were prepared using NP-40 lysis buffer containing protease inhibitor cocktail (Thermo Scientific). Nuclear and cytosolic lysates were prepared using the NucBuster nuclear protein extraction kit (Millipore). Soluble proteins were immunoprecipitated with anti-MUC1-C (NeoMarker) or a control IgG. Immunoprecipitates and lysates not subjected to precipitation were analyzed by immunoblotting with anti-MUC1-C (NeoMarker), anti-CRB3 (Abcam), anti-HUGL2 (Genetex), anti-PATJ, anti-SNAIL1 (Santa Cruz Biotechnology), anti-CDC42, anti-ZEB1, anti-phospho-LATS1, anti-LATS1, anti-phospho-YAP, anti-YAP, anti-HDAC1 (Cell Signaling Technology) and anti- $\beta$ -actin (Sigma). Immunoreactive complexes were detected using horseradish peroxidase-conjugated secondary antibodies (GE Healthcare) and an enhanced chemiluminescence (ECL) detection system (Perkin Elmer Health Sciences).

### Quantitative real time, reverse transcriptase PCR

qRT-PCR analysis was performed on cDNA synthesized from total RNA using the Superscript III cDNA synthesis system (Life Technologies). cDNA samples were then amplified using the SYBR green qPCR assay kit (Applied Biosystems) and the ABI Prism 7300 Sequence Detector (Applied Biosystems)(32). qPCR primers used for detection of CRB3, HUGL2, PATJ, CDC42, CTGF, CYR61, MYC, MUC1 and GAPDH are listed in Supplemental Table S1. Statistical significance was determined by the Student's *t*-test.

### Analysis of CRB3 promoter activity

Cells were cultured in six-well plates followed by transfection with an empty vector, pCRB3-Luc and, as an internal control, *SV-40-Renilla-Luc* (Promega) in the presence of Superfect transfection reagent (Qiagen). After 48 h, the transfected cells were lysed with passive lysis buffer and the lysates were analyzed using the Dual Luciferase Assay system (Promega).

### Chromatin immunoprecipitation (ChIP) assays

Soluble chromatin was prepared from  $2-3 \times 10^6$  cells as described (27) and precipitated with anti-ZEB1, anti- $\beta$ -catenin (Cell Signaling Technology), or a control nonimmune IgG (Santa Cruz Biotechnology). For re-ChIP assays, ZEB1 or  $\beta$ -catenin complexes from the primary ChIP were released and reimmunoprecipitated with anti-MUC1-C (NeoMarker) or anti-YAP (Cell Signaling Technology). The SYBR green qPCR kit (Applied Biosystems) was used for the qPCR analyses with the ABI Prism 7300 Sequence Detector (Applied Biosystems) as described (30, 33). Primer pairs used for the *CRB3* and *MYC* promoters and a control *GAPDH* region are listed in Supplemental Table S2. Relative fold enrichment was calculated as described (34).

### Protein binding assays

GST-tagged YAP, GST-YAP(1-160) and GST-YAP(161-504) were generated by PCR amplification of the GST-YAP plasmid (Addgene) and subcloning into the pGEX-5X-1 expression vector (GE Healthcare). GST- $\beta$ -catenin was expressed from pGEX- $\beta$ -catenin (Addgene) and cleaved with thrombin to isolate purified  $\beta$ -catenin. MUC1-CD, MUC1-CD(1-45) and MUC1-CD(46-72) peptide fragments were prepared by expressing GST-fusion proteins and cleavage of the GST tag with thrombin as described (23). GST and GST fusion proteins bound to glutathione beads were incubated with purified proteins. The adsorbates were analyzed by immunoblotting with anti-MUC1-C cytoplasmic domain antibodies CD1 (35) and CT2 (NeoMarker).

## Results

### MUC1-C downregulates CRB3 expression

BT-549 and MDA-MB-231 Basal B triple-negative breast cancer (TNBC) cells have low to undetectable levels of CRB3, HUGL2 and PATJ expression as compared to that found for CDC42 (Fig. 1A and Fig. 1B). Notably, however, stable silencing of MUC1-C in BT-549 cells was associated with upregulation of CRB3, HUGL2 and PATJ, but not CDC42, mRNA

(Fig. 1A, left) and protein (Fig. 1A, right). We also found that silencing MUC1-C in MDA-MB-231 cells results in induction of CRB3, HUGL2 and PATJ expression (Fig. 1B, left and right), indicating that MUC1-C downregulates multiple effectors of cell polarity. The following studies have focused on CRB3, which in addition to its role in establishing the apical membrane, activates the Hippo pathway (2). Interestingly and in contrast to the results obtained with Basal B TNBC cells, we found that Basal A BT-20 TNBC cells express CRB3 (Fig. 1C, left and right). Moreover, we found that ectopic expression of MUC1-C in BT-20 cells suppresses CRB3 levels (Fig. 1C, left and right). Constitutive expression of CRB3 in epithelial MCF-7 cells was also downregulated by a MUC1-C-mediated mechanism (Supplemental Fig. S1A, left and right). To further assess the regulation of CRB3 in a setting of transiently targeting MUC1-C, we established BT-549 cells transduced to express a tetracycline-inducible MUC1 shRNA (tet-MUC1shRNA). Treatment of BT-549/tet-MUC1shRNA cells with doxycycline (DOX) for 7 days resulted in suppression of MUC1-C and induction of CRB3 expression (Supplemental Fig. S1B, left and right). In contrast, silencing CRB3 had little if any effect on MUC1-C expression (Supplemental Fig. S1D, left and right). The MUC1-C cytoplasmic domain includes a CQC motif that is necessary for the formation of MUC1-C homodimers and their nuclear localization (Fig. 1D) (36–38). Accordingly, we treated BT-549 cells with GO-203, a cell penetrating peptide that targets this CQC motif or, as a control, an inactive peptide CP-2 (18) (Fig. 1D). We found that treatment with GO-203, but not CP-2, results in upregulation of CRB3 mRNA and protein (Fig. 1E, left and right). A similar response was observed when MDA-MB-231 cells were treated with GO-203 (Fig. 1F, left and right). As further evidence, we found that GO-203 blocks MUC1-C-induced CRB3 downregulation in MCF-7/MUC1-C cells (Supplemental Fig. S1C, left and right). These findings support the notion that MUC1-C promotes loss of cell polarity, at least in part, by downregulating CRB3 in a cell context-dependent manner.

### **CRB3 is repressed by a ZEB1-dependent mechanism**

MUC1-C drives ZEB1 expression in BT-549, MDA-MB-231 and MCF-7/MUC1-C cells (23). In turn, MUC1-C binds to ZEB1 and contributes to repression of the ZEB1 target gene, *miR-200c* (23). ZEB1 also represses transcription of the CRB3 gene (39). In this context and to investigate if MUC1-C suppresses CRB3 by a ZEB1-mediated mechanism, we stably silenced ZEB1 in BT-549 cells and found upregulation of CRB3 mRNA and protein (Fig. 2A, left and right). Similar results were obtained with ZEB1 silencing in MDA-MB-231 cells (Fig. 2B, left and right). Moreover, we found that MUC1-C-induced downregulation of CRB3 in MCF-7/MUC1-C cells is ZEB1-dependent (Fig. 2C, left and right). SNAIL1, another transcriptional repressor, binds to the same target *CRB3* promoter region as ZEB1 (39). Silencing MUC1-C in MDA-MB-231 cells was associated with a partial decrease in SNAIL1 expression (Fig. 2D, left); however, silencing SNAIL1 had no apparent effect on CRB3 expression (Fig. 2D, right). Additionally, SNAIL1 was upregulated in MCF-7/MUC1-C cells (Fig. 2E, left) and silencing SNAIL1 had no detectable effect on CRB3 expression in these cells (Fig. 2E, right). These findings supported the premise that MUC1-C suppresses *CRB3* by a ZEB1-dependent, SNAIL1-independent mechanism.

### MUC1-C interacts with ZEB1 on the *CRB3* gene promoter

ZEB1 represses the *CRB3* promoter by binding to five E-Box elements (5'-CACCTG-3') located within 1410 bp upstream to the transcription start site (39)(Fig. 3A). To assess involvement of MUC1-C in suppression of the *CRB3* promoter, we transfected MDA-MB-231 cells with a *CRB3* promoter-luciferase reporter (pCRB3-Luc) containing the proximal 5 E-boxes (Fig. 3A). Silencing MUC1-C was associated with an increase in pCRB3-Luc activity as compared to that found in MDA-MB-231/CshRNA cells (Fig. 3B, left). Similar results were obtained in studies of BT-549 cells (Fig 3B, middle). In addition, overexpression of MUC1-C in MCF-7/MUC1-C cells decreased pCRB3-Luc activity (Fig. 3B, right), indicating that MUC1-C contributes to repression of the *CRB3* promoter. To assess occupancy on the *CRB3* promoter, we performed ChIP and re-ChIP studies on chromatin from MDA-MB-231 cells. The results demonstrated that ZEB1 occupies the *CRB3* promoter (Fig. 3C, left) in a complex with MUC1-C (Fig. 3C, right). Moreover, targeting MUC1-C with GO-203 was associated with a decrease in occupancy of ZEB1 (Fig. 3D, left) and ZEB1/MUC1-C complexes (Fig. 3D, right) on the *CRB3* promoter. Consistent with these results, we found that MUC1-C increases occupancy of ZEB1 (Fig. 3E, left) and ZEB1/MUC1-C complexes (Fig. 3E, right) on the *CRB3* promoter in MCF-7/MUC1-C cells. These findings and those with the pCRB3-Luc reporter support a model in which MUC1-C promotes ZEB1 occupancy on the *CRB3* promoter and thereby inactivates *CRB3* transcription.

### MUC1-C-induced downregulation of *CRB3* results in inactivation of the Hippo pathway

*CRB3* activates the core kinase cassette of the Hippo pathway, which includes MST1/2 and LATS1/2 (5). Activated p-LATS1/2 phosphorylates YAP, which in turn leads to retention of p-YAP in the cytoplasm and its degradation (10, 40). Consistent with activation of the Hippo pathway, silencing MUC1-C in MDA-MB-231 and BT-549 cells was associated with increased p-LATS1 levels (Fig. 4A, left and middle). By contrast, p-LATS1 levels were decreased with overexpression of MUC1-C in MCF-7/MUC1-C cells (Fig. 4A, right). Increases in p-LATS1 were in turn associated with upregulation of p-YAP in the cytosolic fraction of MDA-MB-231/MUC1shRNA (Fig. 4B, left) and BT-549/MUC1shRNA (Fig. 4B, middle) cells. Moreover and in concert with decreases in p-LATS1 in MCF-7/MUC1-C cells, p-YAP was downregulated in the cytosolic fraction (Fig. 4B, right). A concomitant decrease of the transcriptionally active form of non-phosphorylated YAP was observed in the nuclear fraction of MDA-MB-231/MUC1shRNA, as compared with that in MDA-MB-231/CshRNA, cells (Fig. 4C, left). Similar results were obtained in the response to MUC1-C silencing in BT-549 cells (Fig. 4C, middle). In addition, increased levels of nuclear YAP were detectable in MCF/MUC1-C cells (Fig. 4C, right). Activated YAP forms a complex with  $\beta$ -catenin that localizes to the nucleus (10, 11, 14, 15). Moreover, MUC1-C stabilizes  $\beta$ -catenin and promotes activation of WNT/ $\beta$ -catenin/TCF4 target genes (25–27). In concert with these pathways, nuclear  $\beta$ -catenin levels were decreased in MDA-MB-231 and BT-549 cells silenced for MUC1-C as compared to that in control cells (Fig. 4D, left and middle). In contrast, nuclear  $\beta$ -catenin was increased in MCF-7/MUC1-C cells (Fig. 4D, right), supporting a model in which both MUC1-C and YAP may drive nuclear  $\beta$ -catenin signaling.

### MUC1-C binds directly to YAP and $\beta$ -catenin

MUC1-C, like YAP, binds directly to  $\beta$ -catenin (24, 25). We therefore asked if MUC1-C forms a complex with YAP and  $\beta$ -catenin. Coimmunoprecipitation studies using lysates from MDA-MB-231 cells showed that MUC1-C associates with YAP (Fig. 5A, left). Similar results were obtained with BT-549 and MCF-7/MUC1-C cells (Fig. 5A, middle and right). To further define the interaction between MUC1-C and YAP, we incubated GST-YAP with purified MUC1-C cytoplasmic domain (MUC1-CD) and found direct binding (Fig. 5B). We also found that GST-YAP(1–160), but not GST-YAP(161–504), binds to MUC1-CD (Fig. 5C). In addition, GST-YAP binds to purified MUC1-CD(1–45) and not MUC1-CD(46–72) (Fig. 5D). Based on these findings and our previous work that MUC1-CD binds to  $\beta$ -catenin (24, 25), we incubated GST-YAP with purified MUC1-CD and  $\beta$ -catenin. Interestingly, the results demonstrate that MUC1-CD promotes the formation of trimolecular complexes containing both YAP and  $\beta$ -catenin (Fig. 5E).

### MUC1-C associates with YAP and $\beta$ -catenin on the *MYC* promoter

YAP activates Hippo target genes by forming transcriptional complexes with TEAD family members and with  $\beta$ -catenin/TCF4 (4). Based on the findings that MUC1-C activates YAP, we first asked if MUC1-C signaling is linked to YAP/TEAD-driven genes, such as *CTGF* and *CYR61*. Indeed, we found that targeting MUC1-C suppresses *CTGF* and *CYR61* expression (Fig. 6A), indicating that MUC1-C promotes activation of this arm of YAP-activated transcription. The interaction between YAP and  $\beta$ -catenin also promotes activation of their respective target genes (11, 14, 15, 41). Recent work has demonstrated that MUC1-C drives *MYC* expression by forming complexes with  $\beta$ -catenin on the *MYC* promoter and increasing  $\beta$ -catenin occupancy (27, 28). Other studies have supported a role for YAP/ $\beta$ -catenin in activating *MYC* expression (42). These and the above findings that MUC1-C forms a complex with YAP and  $\beta$ -catenin invoked the possibility that MUC1-C could associate with YAP and  $\beta$ -catenin on the *MYC* promoter. To investigate this notion, we performed ChIP and re-ChIP studies of the *MYC* promoter in MDA-MB-231 cells. We found that  $\beta$ -catenin occupies the *MYC* promoter (Fig. 6B) and that  $\beta$ -catenin associates with both MUC1-C and YAP (Fig. 6B). To determine whether the formation of these complexes is MUC1-C-dependent, we targeted MUC1-C with GO-203 treatment. The results showed that targeting MUC1-C is associated with decreased  $\beta$ -catenin occupancy on the *MYC* promoter (Fig. 6C). Moreover, in re-ChIP studies, we found that GO-203 treatment is associated with decreases in MUC1-C and YAP occupancy (Fig. 6C). In addition, targeting MUC1-C with GO-203 (Fig. 6D, left and right) or silencing (Fig. 6E, left and right) resulted in the suppression of *MYC* mRNA and protein. As confirmation that the observed *MYC* downregulation is indeed YAP-dependent, we transiently silenced YAP in MDA-MB-231 cells and found suppression of *MYC* expression (Fig. 6F).

## Discussion

Epithelia are comprised of a single layer of cells that have a unique structure in which the apical surface faces (i) the external environment in the respiratory and gastrointestinal tracts, or (ii) a lumen in ducts of specialized organs, such as the mammary gland (Fig. 7A)(2). Apical-basal polarity is however disrupted in the response to stress and is associated with

induction of a proliferation and survival program (43). MUC1 evolved in mammals to afford protection of epithelia (16, 44). In this way, the MUC1-N subunit forms a physical mucous barrier that protects against agents, such as toxins and microorganisms among others, that damage the apical surface (Fig. 7A) (16). In turn, the MUC1-C subunit functions in transducing signals that promote the growth and survival response (Fig. 7A) (16). The present studies provide evidence that MUC1-C is of importance to the loss of epithelial cell polarity. Our results demonstrate that MUC1-C drives downregulation of (i) the Scribble complex HUGL2 protein, which is necessary for the establishment of the basolateral domains, and (ii) the Crumbs complex CRB3 and PATJ proteins, which define the apical membrane (2). The Scribble and Crumbs complexes are necessary for maintaining apical-basal polarity and epithelial integrity. These findings do not exclude the possibility that MUC1-C regulates other effectors necessary for cell polarity. In this regard, MUC1-C (i) epigenetically suppresses *CDHI* expression, which disrupts adherens junctions, and (ii) interacts directly with  $\beta$ -catenin and p120, promoting their import from the lateral cell membrane to the nucleus (16, 17). Collectively, these findings support a previously unidentified model in which MUC1-C induces loss of polarity and integrates that response with self-renewal and stemness (21). In concert with this model, MUC1-C is expressed over the entire surface of breast cancer cells and is substantially upregulated (45), supporting the premise that TNBC cells have appropriated and exploited MUC1-C to confer properties of EMT, invasion and self-renewal (Fig. 7B) (21, 23).

MUC1-C activates the inflammatory NF- $\kappa$ B pathway through interactions with TAK1 and the IKKs (33, 46). In addition, MUC1-C binds directly to NF- $\kappa$ B p65 and increases NF- $\kappa$ B occupancy on the promoters of its target genes, including *MUC1* itself in an autoinductive circuit (22). The MUC1-C $\rightarrow$ NF- $\kappa$ B pathway also drives the *ZEB1* gene (23), which encodes a transcriptional repressor that promotes EMT (47). In turn, MUC1-C forms a complex with ZEB1 and confers ZEB1 occupancy on *miR-200c* promoter and thereby its suppression (23). The present results further demonstrate that MUC1-C/ZEB1 complexes occupy the *CRB3* promoter and, like *miR-200c*, inhibit *CRB3* transcription (Fig. 7B, left). A similar mechanism of suppression applies to the *HUGL2* promoter, linking MUC1-C/ZEB1 complexes to the downregulation of the *CRB3* and *HUGL2* genes. ZEB1 also plays a role in suppressing expression of the Pals1-associated tight junction protein (39); however, further studies will be needed to assess whether MUC1-C is also involved in this pathway. Indeed and as mentioned above, the present work has focused on MUC1-C-induced downregulation of CRB3 as a potential mechanism by which MUC1-C integrates loss of polarity and EMT with the Hippo pathway. By extension, the Hippo pathway regulates proliferation, apoptosis and differentiation (4, 5, 48), all of which have also been ascribed to MUC1-C signaling (16, 17). In concert with CRB3 functioning as an activator of the Hippo pathway, we found that targeting MUC1-C in TNBC cells is associated with increases in p-LATS1. In further support of MUC1-C as an inhibitor of the Hippo pathway, ectopic expression of MUC1-C in MCF-7 cells decreased p-LATS1. These findings support a model in which MUC1-C constitutively suppresses CRB3 and the Hippo pathway in mesenchymal TNBC cells. In addition, overexpression of MUC1-C in luminal MCF-7 cells is necessary for induction of these responses, indicating that this MUC1-C function is at least in part dependent on cell context. In this regard, MUC1-C activates the inflammatory NF- $\kappa$ B pathway in



mesenchymal breast cancer cells, which also have increased YAP activity (49). By contrast, in luminal MCF-7 cells, ectopic MUC1-C expression is necessary for activating the NF- $\kappa$ B pathway (21, 23). These findings and the present results provide evidence that MUC1-C links the NF- $\kappa$ B inflammatory response to loss of polarity and suppression of the Hippo pathway (Figs. 7B, left).

One outcome of an activated Hippo pathway is p-LATS1-mediated phosphorylation of YAP, resulting in the retention of p-YAP in the cytoplasm (10). By contrast, activated YAP localizes to the nucleus, where it functions by associating with transcription factors, such as TEAD (TEA domain family member) and  $\beta$ -catenin/TCF4, to activate genes involved in tumor induction and progression (4, 10). Another mechanism by which CRB3 can direct Hippo pathway function is by sequestering p-YAP at cell junctions through formation of complexes with certain cell polarity proteins, such as PALS, PATJ and AMOT. This sequestration also prevents access of p-YAP to phosphatases that counter the effect of the Hippo pathway kinases on YAP phosphorylation (4, 6). The present studies demonstrate that MUC1-C downregulates the Hippo pathway and thereby induces the nuclear localization of activated YAP (Figs. 7B, right). In the nucleus, YAP functions as a co-activator involved in the regulation of transcriptional programs that determine organ size and promote cellular proliferation (10). YAP has also been linked to transformation by activating transcription of mitogenic and anti-apoptotic genes through interactions with TEAD or with  $\beta$ -catenin/TCF4 (10, 11, 13–15). MUC1-C activates the WNT/ $\beta$ -catenin pathway by stabilizing  $\beta$ -catenin and driving WNT target genes, such as *CCND1* and *MYC* (25–28). The present work extends this interaction by demonstrating that the MUC1-C cytoplasmic domain binds directly to YAP and promotes the *in vitro* formation of YAP/ $\beta$ -catenin complexes. In addition, we found that (i) MUC1-C associates with  $\beta$ -catenin and YAP on the *MYC* promoter, and (ii) targeting MUC1-C decreases occupancy of both  $\beta$ -catenin and YAP (Fig. 7B, right). In concert with these findings, targeting MUC1-C resulted in the downregulation of *MYC*, which in turn affects multiple pathways involved in cell growth, proliferation and survival (50).

In summary, our findings provide convincing evidence for a previously unidentified role for MUC1-C in promoting loss of apical-basal polarity and linking this response to regulation of the Hippo pathway and YAP activation (Fig. 7B). These studies have largely focused on TNBC cells; however, we note that the results may be more broadly applicable to other types of carcinomas with overexpression of MUC1-C and downregulation of CRB3. Our findings also provide support for the notion that MUC1-C is an attractive therapeutic target. In this regard, GO-203 has completed Phase I clinical evaluation and has been formulated in polymeric nanoparticles for the treatment of patients with TNBC and other MUC1-C-expressing cancers (51).

## Supplementary Material

Refer to Web version on PubMed Central for supplementary material.

## Acknowledgments

**Financial Support:** Research reported in this publication was supported by the National Cancer Institute of the National Institutes of Health under award numbers CA97098 and CA166480 and the Lung Cancer Research Foundation.

## Abbreviations

<b>MUC1</b>	mucin 1
<b>MUC1-C</b>	MUC1 C-terminal transmembrane subunit
<b>CRB3</b>	mammalian homolog 3 of <i>Drosophila</i> Crumbs (Crb)
<b>TNBC</b>	triple-negative breast cancer
<b>YAP</b>	Yes-associated protein
<b>TAZ</b>	the transcriptional co-activator with PDZ-binding motif
<b>TSG</b>	Tumor Suppressor Gene
<b>ChIP</b>	chromatin immunoprecipitation
<b>DOX</b>	doxycycline
<b>TEAD</b>	transcriptional enhancer activator domain family of transcription factors

## References

1. Thiery JP, Acloque H, Huang RY, Nieto MA. Epithelial-mesenchymal transitions in development and disease. *Cell*. 2009; 139(5):871–90. [PubMed: 19945376]
2. Martin-Belmonte F, Perez-Moreno M. Epithelial cell polarity, stem cells and cancer. *Nat Rev Cancer*. 2012; 12(1):23–38.
3. Moreno-Bueno G, Portillo F, Cano A. Transcriptional regulation of cell polarity in EMT and cancer. *Oncogene*. 2008; 27(55):6958–69. [PubMed: 19029937]
4. Harvey KF, Zhang X, Thomas DM. The Hippo pathway and human cancer. *Nat Rev Cancer*. 2013; 13(4):246–57. [PubMed: 23467301]
5. Meng Z, Moroishi T, Guan KL. Mechanisms of Hippo pathway regulation. *Genes Dev*. 2016; 30(1): 1–17. [PubMed: 26728553]
6. Mo JS, Park HW, Guan KL. The Hippo signaling pathway in stem cell biology and cancer. *EMBO Rep*. 2014; 15(6):642–56. [PubMed: 24825474]
7. Pefani DE, O'Neill E. Hippo pathway and protection of genome stability in response to DNA damage. *FEBS J*. 2015
8. Maugeri-Sacca M, De Maria R. Hippo pathway and breast cancer stem cells. *Crit Rev Oncol Hematol*. 2016; 99:115–22. [PubMed: 26725175]
9. Varelas X, Miller BW, Sopko R, et al. The Hippo pathway regulates Wnt/beta-catenin signaling. *Dev Cell*. 2010; 18(4):579–91. [PubMed: 20412773]
10. Moroishi T, Hansen CG, Guan KL. The emerging roles of YAP and TAZ in cancer. *Nat Rev Cancer*. 2015; 15(2):73–9. [PubMed: 25592648]
11. Heallen T, Zhang M, Wang J, et al. Hippo pathway inhibits Wnt signaling to restrain cardiomyocyte proliferation and heart size. *Science*. 2011; 332(6028):458–61. [PubMed: 21512031]
12. Pan D. The hippo signaling pathway in development and cancer. *Dev Cell*. 2010; 19(4):491–505. [PubMed: 20951342]

13. Kim M, Jho EH. Cross-talk between Wnt/beta-catenin and Hippo signaling pathways: a brief review. *BMB Rep.* 2014; 47(10):540–5. [PubMed: 25154721]
14. Imajo M, Miyatake K, Imura A, Miyamoto A, Nishida E. A molecular mechanism that links Hippo signalling to the inhibition of Wnt/beta-catenin signalling. *EMBO J.* 2012; 31(5):1109–22. [PubMed: 22234184]
15. Tao J, Calvisi DF, Ranganathan S, et al. Activation of beta-catenin and Yap1 in human hepatoblastoma and induction of hepatocarcinogenesis in mice. *Gastroenterology.* 2014; 147(3): 690–701. [PubMed: 24837480]
16. Kufe D. Mucins in cancer: function, prognosis and therapy. *Nature Reviews Cancer.* 2009; 9(12): 874–85. [PubMed: 19935676]
17. Kufe D. MUC1-C oncoprotein as a target in breast cancer: activation of signaling pathways and therapeutic approaches. *Oncogene.* 2013; 32(9):1073–81. [PubMed: 22580612]
18. Raina D, Kosugi M, Ahmad R, et al. Dependence on the MUC1-C oncoprotein in non-small cell lung cancer cells. *Mol Cancer Ther.* 2011; 10(5):806–16. [PubMed: 21421804]
19. Raina D, Uchida Y, Kharbanda A, et al. Targeting the MUC1-C oncoprotein downregulates HER2 activation and abrogates trastuzumab resistance in breast cancer cells. *Oncogene.* 2014; 33(26): 3422–31. [PubMed: 23912457]
20. Alam M, Ahmad R, Rajabi H, Kharbanda A, Kufe D. MUC1-C oncoprotein activates ERK→C/EBPβ-mediated induction of aldehyde dehydrogenase activity in breast cancer cells. *J Biol Chem.* 2013; 288(43):30829–903.
21. Alam M, Rajabi H, Ahmad R, Jin C, Kufe D. Targeting the MUC1-C oncoprotein inhibits self-renewal capacity of breast cancer cells. *Oncotarget.* 2014; 5(9):2622–34. [PubMed: 24770886]
22. Ahmad R, Raina D, Joshi MD, Kawano T, Kharbanda S, Kufe D. MUC1-C oncoprotein functions as a direct activator of the NF-κB p65 transcription factor. *Cancer Res.* 2009; 69:7013–21. [PubMed: 19706766]
23. Rajabi H, Alam M, Takahashi H, et al. MUC1-C oncoprotein activates the ZEB1/miR-200c regulatory loop and epithelial-mesenchymal transition. *Oncogene.* 2014; 33(13):1680–9. [PubMed: 23584475]
24. Yamamoto M, Bharti A, Li Y, Kufe D. Interaction of the DF3/MUC1 breast carcinoma-associated antigen and β-catenin in cell adhesion. *J Biol Chem.* 1997; 272(19):12492–4. [PubMed: 9139698]
25. Huang L, Chen D, Liu D, Yin L, Kharbanda S, Kufe D. MUC1 oncoprotein blocks GSK3β-mediated phosphorylation and degradation of β-catenin. *Cancer Res.* 2005; 65(22):10413–22. [PubMed: 16288032]
26. Rajabi H, Ahmad R, Jin C, et al. MUC1-C oncoprotein induces TCF7L2 transcription factor activation and promotes cyclin D1 expression in human breast cancer cells. *J Biol Chem.* 2012; 287(13):10703–13. [PubMed: 22318732]
27. Bouillez A, Rajabi H, Pitroda S, et al. Inhibition of MUC1-C suppresses MYC expression and attenuates malignant growth in KRAS mutant lung adenocarcinomas. *Cancer Res.* 2016; 76(6): 1538–48. [PubMed: 26833129]
28. Tagde A, Rajabi H, Bouillez A, et al. MUC1-C drives MYC in multiple myeloma. *Blood.* 2016; 127(21):2587–97. [PubMed: 26907633]
29. Kharbanda A, Rajabi H, Jin C, Alam M, Wong K, Kufe D. MUC1-C confers EMT and KRAS independence in mutant KRAS lung cancer cells. *Oncotarget.* 2014; 5(19):8893–905. [PubMed: 25245423]
30. Hasegawa M, Takahashi H, Rajabi H, et al. Functional interactions of the cystine/glutamate antiporter, CD44v and MUC1-C oncoprotein in triple-negative breast cancer cells. *Oncotarget.* 2016; 7(11):11756–69. [PubMed: 26930718]
31. Hiraki M, Suzuki Y, Alam M, et al. MUC1-C stabilizes MCL-1 in the oxidative stress response of triple-negative breast cancer cells to BCL-2 inhibitors. *Sci Rep.* 2016:6.
32. Sonawane P, Cho HE, Tagde A, et al. Metabolic characteristics of 13-cis-retinoic acid (isotretinoin) and anti-tumour activity of the 13-cis-retinoic acid metabolite 4-oxo-13-cis-retinoic acid in neuroblastoma. *Br J Pharmacol.* 2014; 171(23):5330–44. [PubMed: 25039756]
33. Takahashi H, Jin C, Rajabi H, et al. MUC1-C activates the TAK1 inflammatory pathway in colon cancer. *Oncogene.* 2015; 34(40):5187–97. [PubMed: 25659581]

34. Wang Q, Carroll JS, Brown M. Spatial and temporal recruitment of androgen receptor and its coactivators involves chromosomal looping and polymerase tracking. *Mol Cell*. 2005; 19(5):631–42. [PubMed: 16137620]
35. Panchamoorthy G, Rehan H, Kharbanda A, Ahmad R, Kufe D. A monoclonal antibody against the oncogenic mucin 1 cytoplasmic domain. *Hybridoma*. 2011; 30(6):531–5. [PubMed: 22149278]
36. Leng Y, Cao C, Ren J, et al. Nuclear import of the MUC1-C oncoprotein is mediated by nucleoporin Nup62. *J Biol Chem*. 2007; 282(27):19321–30. [PubMed: 17500061]
37. Raina D, Ahmad R, Rajabi H, Panchamoorthy G, Kharbanda S, Kufe D. Targeting cysteine-mediated dimerization of the MUC1-C oncoprotein in human cancer cells. *Int J Oncol*. 2012; 40(5):1643–9. [PubMed: 22200620]
38. Raina D, Agarwal P, Lee J, et al. Characterization of the MUC1-C cytoplasmic domain as a cancer target. *PLoS One*. 2015; 10(8):e0135156. [PubMed: 26267657]
39. Aigner K, Dampier B, Descovich L, et al. The transcription factor ZEB1 ( $\Delta$ EF1) promotes tumour cell dedifferentiation by repressing master regulators of epithelial polarity. *Oncogene*. 2007; 26(49):6979–88. [PubMed: 17486063]
40. Zhao B, Wei X, Li W, et al. Inactivation of YAP oncoprotein by the Hippo pathway is involved in cell contact inhibition and tissue growth control. *Genes Dev*. 2007; 21(21):2747–61. [PubMed: 17974916]
41. Rosenbluh J, Nijhawan D, Cox AG, et al. beta-Catenin-driven cancers require a YAP1 transcriptional complex for survival and tumorigenesis. *Cell*. 2012; 151(7):1457–73. [PubMed: 23245941]
42. Shao DD, Xue W, Krall EB, et al. KRAS and YAP1 converge to regulate EMT and tumor survival. *Cell*. 2014; 158(1):171–84. [PubMed: 24954536]
43. Vermeer PD, Einwalter LA, Moninger TO, et al. Segregation of receptor and ligand regulates activation of epithelial growth factor receptor. *Nature*. 2003; 422(6929):322–6. [PubMed: 12646923]
44. Duraisamy S, Kufe T, Ramasamy S, Kufe D. Evolution of the human MUC1 oncoprotein. *Int J Oncology*. 2007; 31:671–7.
45. Kufe D, Inghirami G, Abe M, Hayes D, Justi-Wheeler H, Schlom J. Differential reactivity of a novel monoclonal antibody (DF3) with human malignant versus benign breast tumors. *Hybridoma*. 1984; 3(3):223–32. [PubMed: 6094338]
46. Ahmad R, Raina D, Trivedi V, et al. MUC1 oncoprotein activates the I $\kappa$ B kinase  $\beta$  complex and constitutive NF- $\kappa$ B signaling. *Nat Cell Biol*. 2007; 9:1419–27. [PubMed: 18037881]
47. Brabletz S, Brabletz T. The ZEB/miR-200 feedback loop—a motor of cellular plasticity in development and cancer? *EMBO Rep*. 2010; 11(9):670–7. [PubMed: 20706219]
48. McCaffrey LM, Macara IG. Epithelial organization, cell polarity and tumorigenesis. *Trends Cell Biol*. 2011; 21(12):727–35. [PubMed: 21782440]
49. Cordenonsi M, Zanconato F, Azzolin L, et al. The Hippo transducer TAZ confers cancer stem cell-related traits on breast cancer cells. *Cell*. 2011; 147(4):759–72. [PubMed: 22078877]
50. Dang CV. MYC on the path to cancer. *Cell*. 2012; 149(1):22–35. [PubMed: 22464321]
51. Hasegawa M, Sinha RK, Kumar M, et al. Intracellular targeting of the oncogenic MUC1-C protein with a novel GO-203 nanoparticle formulation. *Clin Cancer Res*. 2015; 21(10):2338–47. [PubMed: 25712682]

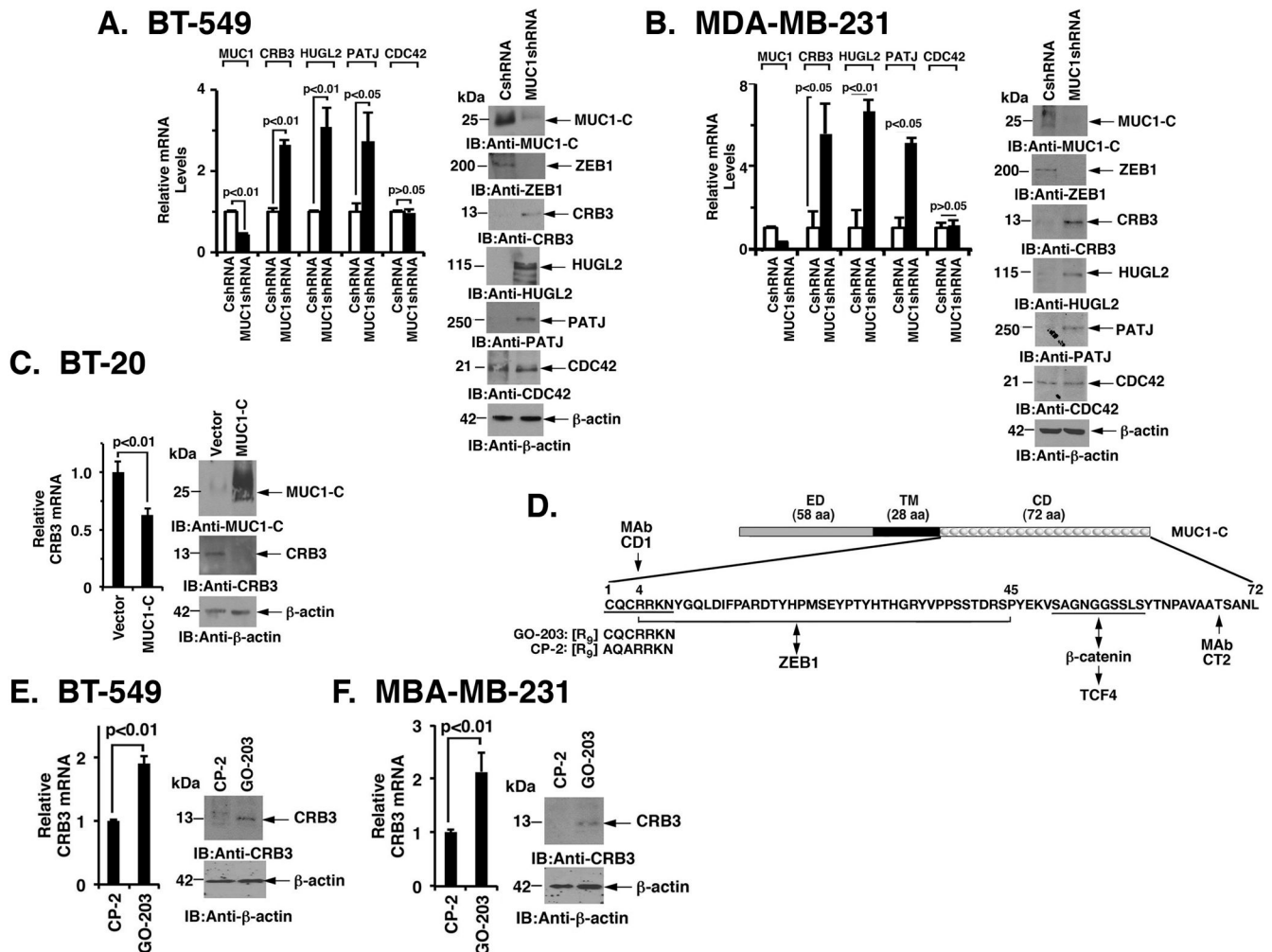


**Figure 1. MUC1-C downregulates CRB3 expression**

A, BT-549 cells infected with lentiviruses to stably express a control scrambled shRNA (CshRNA) or a MUC1shRNA were analyzed for MUC1, CRB3, HUGL2, PATJ and CDC42 mRNA levels by qRT-PCR (left). The results are expressed as relative mRNA levels (mean  $\pm$ SD of three determinations) as compared with that obtained for BT-549/CshRNA cells (assigned a value of 1). Lysates from the BT-549/CshRNA and BT-549/MUC1shRNA cells were immunoblotted with the indicated antibodies (right). B, MDA-MB-231/CshRNA and MDA-MB-231/MUC1shRNA cells were analyzed for MUC1, CRB3, HUGL2, PATJ and CDC42 mRNA levels by qRT-PCR (left). The results are expressed as relative mRNA levels (mean  $\pm$ SD of three determinations) as compared with that obtained for MDA-MB-231/CshRNA cells (assigned a value of 1). Lysates from the MDA-MB-231/CshRNA and MDA-MB-231/MUC1shRNA cells were immunoblotted with the indicated antibodies (right). C, BT-20 cells stably expressing an empty vector or MUC1-C were analyzed for CRB3 mRNA levels by qRT-PCR (left). The results are expressed as relative CRB3 mRNA levels (mean  $\pm$ SD of three determinations) as compared to that obtained for BT-20/vector cells (assigned a value of 1). Lysates from the BT-20/vector and BT-20/MUC1-C cells were immunoblotted with the indicated antibodies (right). D, Schematic showing the MUC1-C subunit and the

amino acid (aa) sequence of the cytoplasmic domain (CD). ED, extracellular domain; TM, transmembrane domain. The CQC motif is necessary and sufficient for MUC1-C homodimerization. D-amino acid sequences are shown for GO-203 and CP-2. E, BT-549 cells were treated with 5  $\mu$ M GO-203 or CP-2 each day for 3 days and then analyzed for CRB3 mRNA levels by qRT-PCR (left). Lysates from BT-549 cells treated as above were immunoblotted with the indicated antibodies (right). F, MDA-MB-231 cells were treated with 5  $\mu$ M GO-203 or CP-2 each day for 3 days and then analyzed for CRB3 mRNA levels by qRT-PCR (left), while lysates from similarly treated cells were immunoblotted with the indicated antibodies (right).

Author Manuscript

Author Manuscript

Author Manuscript

Author Manuscript

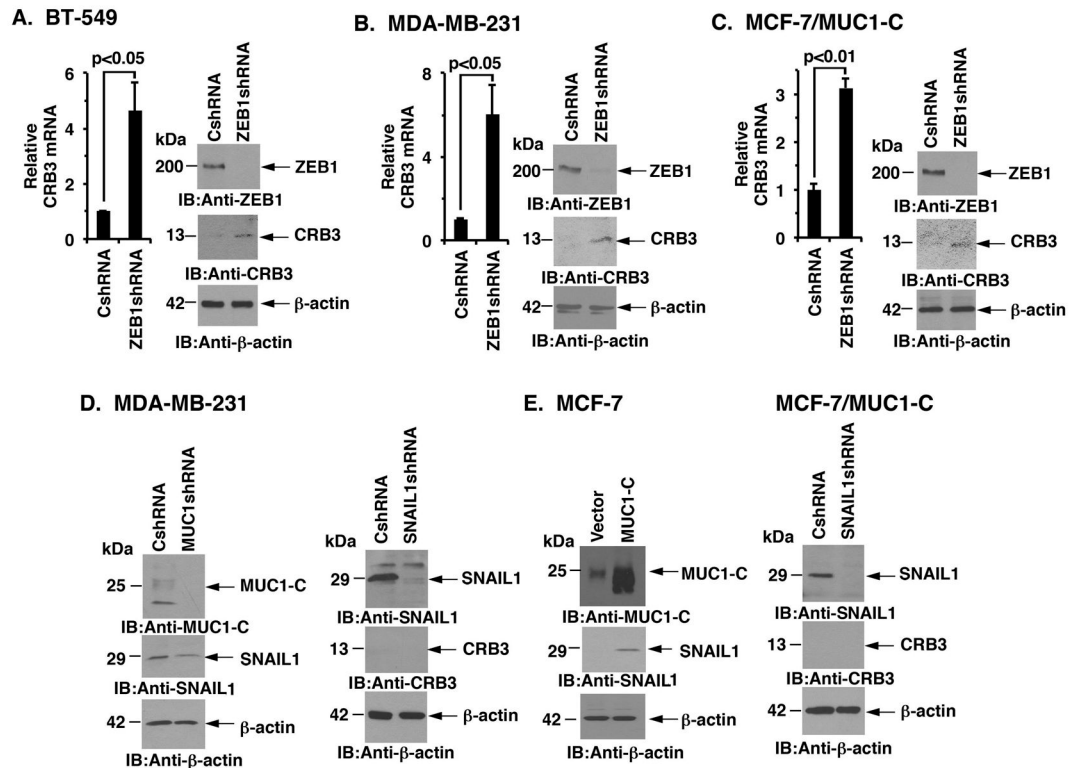


**Figure 2. MUC1-C suppresses CRB3 expression by a ZEB1-dependent mechanism**

A, BT-549 cells infected with lentiviruses to stably express a control scrambled shRNA (CshRNA) or a ZEB1shRNA were analyzed for CRB3 mRNA levels by qRT-PCR (left). The results are expressed as relative CRB3 mRNA levels (mean±SD of three determinations) as compared with that obtained for BT-549/CshRNA cells (assigned a value of 1). Lysates from the BT-549/CshRNA and BT-549/ZEB1shRNA cells were immunoblotted with the indicated antibodies (right). B, MDA-MB-231 cells stably expressing a control scrambled shRNA (CshRNA) or a ZEB1 shRNA were analyzed for CRB3 mRNA levels by qRT-PCR (left). The results are expressed as relative CRB3 mRNA levels (mean±SD of three determinations) as compared with that obtained for MDA-MB-231/CshRNA cells (assigned a value of 1). Lysates from the MDA-MB-231/CshRNA and MDA-MB-231/ZEB1shRNA cells were immunoblotted with the indicated antibodies (right). C, MCF-7/MUC1-C cells stably expressing a control scrambled shRNA (CshRNA) or a ZEB1 shRNA were analyzed for CRB3 mRNA levels by qRT-PCR (left). Lysates from MCF-7/MUC1-C/CshRNA and MCF-7/MUC1-C/ZEB1shRNA cells were immunoblotted with the indicated antibodies (right). D, Lysates from MDA-MB-231/CshRNA and MDA-MB-231/MUC1shRNA (left) and from MDA-MB-231/CshRNA and MDA-MB-231/SNAIL1shRNA (right) cells were immunoblotted with the indicated antibodies. E, Lysates from MCF-7/vector and MCF-7/MUC1-C cells (left) were immunoblotted with the indicated antibodies. Lysates from MCF-7/MUC1-C cells infected with lentiviruses to stably express a control scrambled shRNA (CshRNA) or a SNAIL1shRNA were immunoblotted with the indicated antibodies (right).

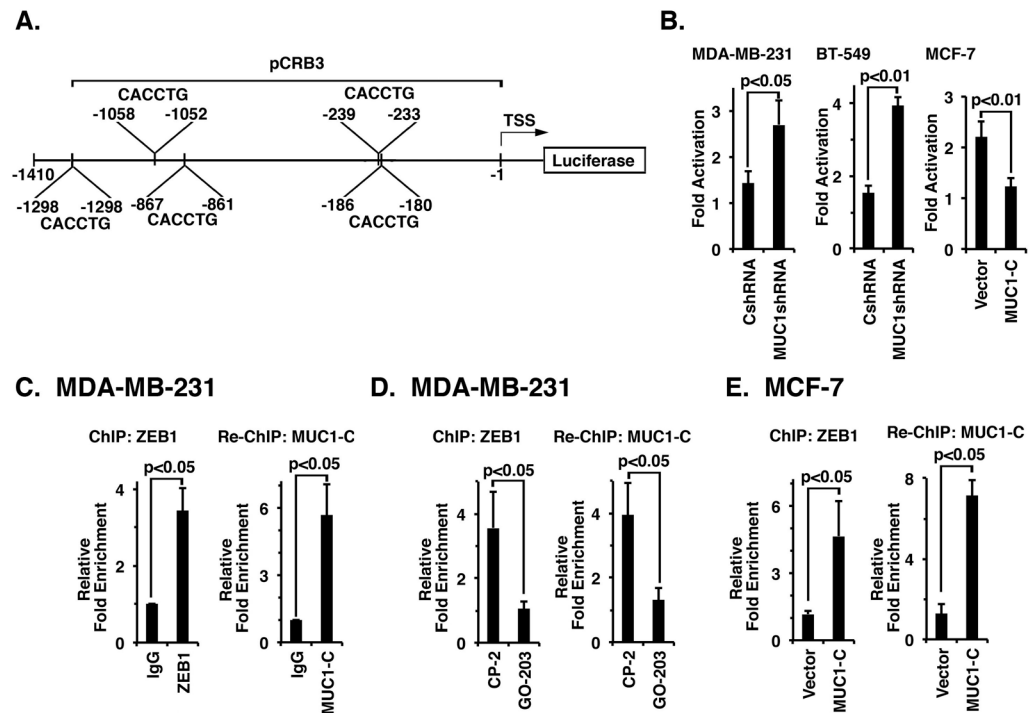


**Figure 3. MUC1-C represses CRB3 promoter activation by a ZEB1-dependent mechanism**

A, Schema of CRB3 luciferase reporter plasmid. B, MDA-MB-231/CshRNA and MDA-MB-231/MUC1shRNA cells (left), BT-549/CshRNA and BT-549/MUC1shRNA cells (middle) and MCF-7/Vector and MCF-7/MUC1-C cells (right) were transfected with the empty Luc vector or pCRB3-Luc. Cells were also transfected with the SV-40-Renilla-Luc plasmid as an internal control. Luciferase activity was measured at 48 h following transfection. The results are expressed as relative luciferase activity (mean $\pm$ SD of three determinations) compared with that obtained from cells transfected with the empty Luc vector (assigned a value of 1). C (left), Soluble chromatin from the indicated MDA-MB-231 cells was precipitated with anti-ZEB1 or a control IgG. The final DNA precipitates were amplified by qPCR with pairs of primers for the ZEB1 binding region in CRB3 promoter region. Results are expressed as the relative fold enrichment (mean $\pm$ SD of three determinations) compared with that obtained for the IgG control (assigned a value of 1). For re-ChIP analysis, soluble chromatin from MDA-MB-231 cells (right) was first precipitated with anti-ZEB1, then released and reimmunoprecipitated with anti-MUC1-C. The results are expressed as the relative fold enrichment (mean $\pm$ SD of three determinations) compared with that obtained with the IgG control (assigned a value of 1). D, MDA-MB-231 cells were treated with 5  $\mu$ M GO-203 or CP-2 each day for 3 days. Soluble chromatin was precipitated with anti-ZEB1 or a control IgG (left). For re-ChIP analysis, complexes were released and re-immunoprecipitated with anti-MUC1-C (right). Results are expressed as the relative fold enrichment (mean $\pm$ SD of three determinations) compared with that obtained for the IgG control (assigned a value of 1). E, Soluble chromatin from MCF-7/vector and MCF-7/MUC1-C cells was precipitated with anti-ZEB1 or a control IgG (left). For re-ChIP analysis, complexes were released and re-immunoprecipitated with anti-MUC1-C (right). Results are



expressed as the relative fold enrichment (mean $\pm$ SD of three determinations) compared with that obtained for the IgG control (assigned a value of 1).

Author Manuscript

Author Manuscript

Author Manuscript

Author Manuscript

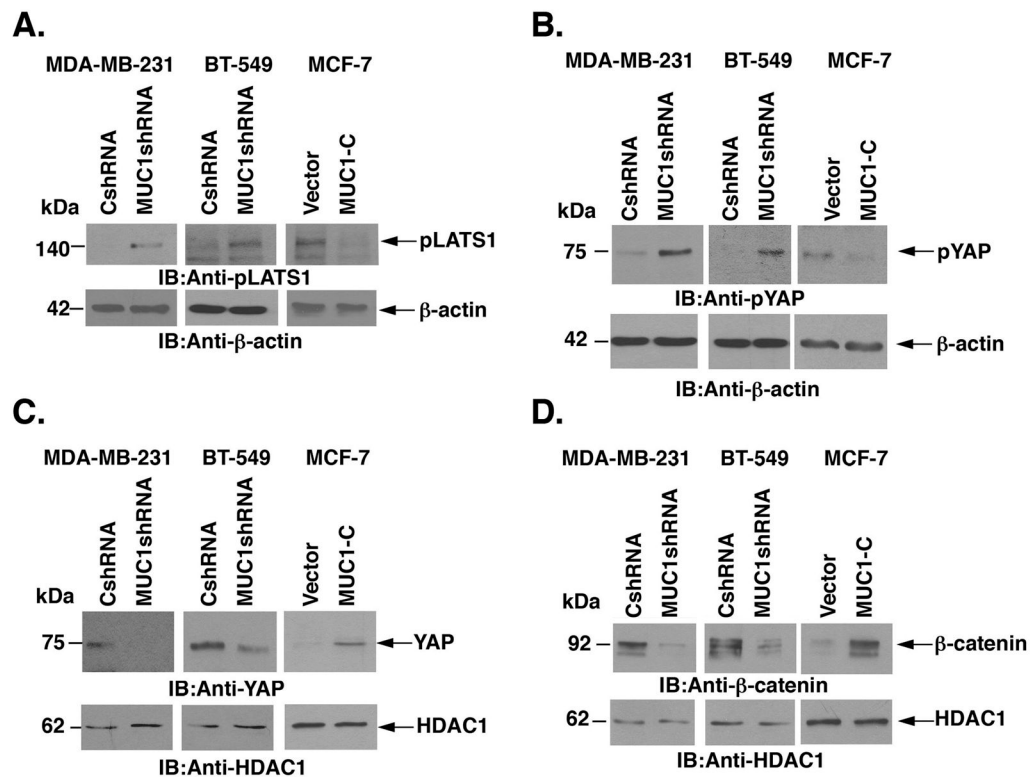


**Figure 4. MUC1-C-mediated CRB3 repression increases nuclear accumulation of YAP**

A, Lysates from MDA-MB-231/CshRNA and MDA-MB-231/MUC1shRNA cells (left), BT-549/CshRNA and BT-549/MUC1shRNA (middle) and MCF-7/Vector and MCF-7/MUC1-C (right) were immunoblotted with the indicated antibodies. B, Cytosolic fraction from MDA-MB-231/CshRNA and MDA-MB-231/MUC1shRNA cells (left), BT-549/CshRNA and BT-549/MUC1shRNA (middle) and MCF-7/Vector and MCF-7/MUC1-C (right) were immunoblotted with the indicated antibodies. C, Nuclear fraction lysates from MDA-MB-231/CshRNA and MDA-MB-231/MUC1shRNA cells (left), BT-549/CshRNA and BT-549/MUC1shRNA (middle) and MCF-7/Vector and MCF-7/MUC1-C (right) were immunoblotted with the indicated antibodies. D, Nuclear fraction lysates from MDA-MB-231/CshRNA and MDA-MB-231/MUC1shRNA cells (left), BT-549/CshRNA and BT-549/MUC1shRNA (middle) and MCF-7/Vector and MCF-7/MUC1-C (right) were immunoblotted with the indicated antibodies.

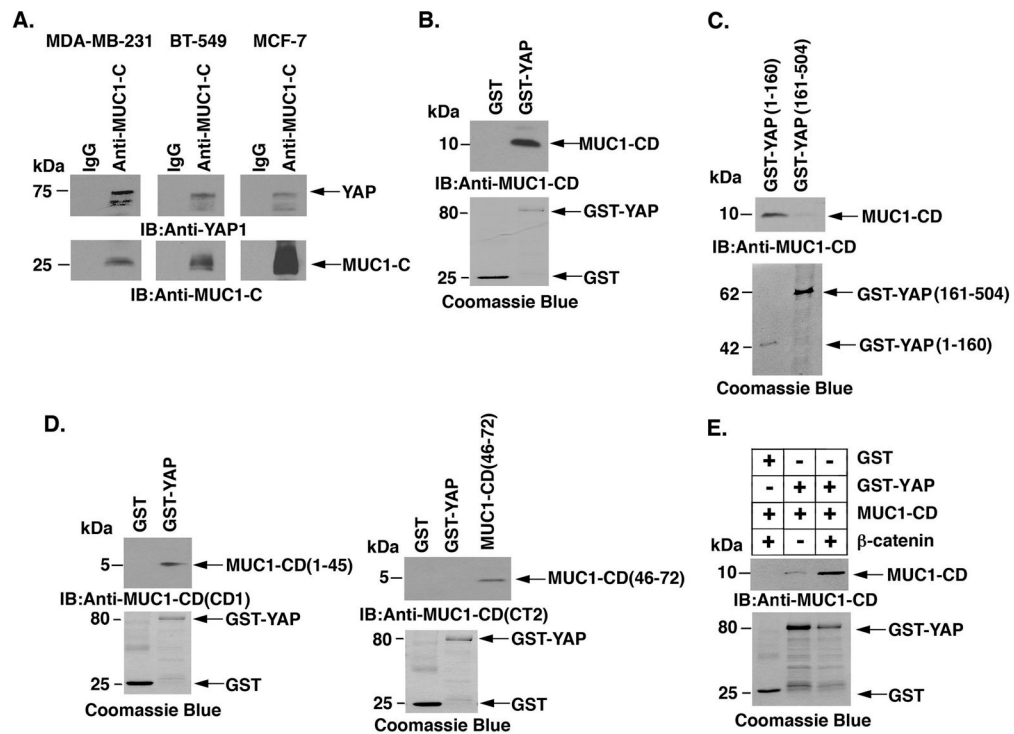


**Figure 5. Binding of MUC1-C and YAP**

A, Lysates from MDA-MB- 231 (left), BT-549 (middle) and MCF-7/MUC1-C (right) cells were precipitated with anti-MUC1-C or a control IgG. The precipitates were immunoblotted with the indicated antibodies. B, GST and GST-YAP were incubated with purified MUC1-C cytoplasmic domain (MUC1-CD). The adsorbates were immunoblotted with anti-MUC1-C. Input of the GST proteins was assessed by Coomassie blue staining. C, GST-YAP(1–160) and GST-YAP(161–504) were incubated with purified MUC1-CD. The adsorbates were immunoblotted with anti-MUC1-C. Input of the GST proteins was assessed by Coomassie blue staining. D, GST and GST-YAP were incubated with MUC1-CD(1–45) (left) or MUC1-CD(46–72) (right). The adsorbates and purified MUC1-CD proteins were immunoblotted with anti-MUC1-CD (CD1, left; CT2, right) antibodies. Input of the GST proteins was assessed by Coomassie blue staining. E, GST and GST-YAP were incubated with purified MUC1-CD and/or with purified  $\beta$ -catenin. The adsorbates were immunoblotted with anti-MUC1-CD. Input of the GST proteins was assessed by Coomassie blue staining.

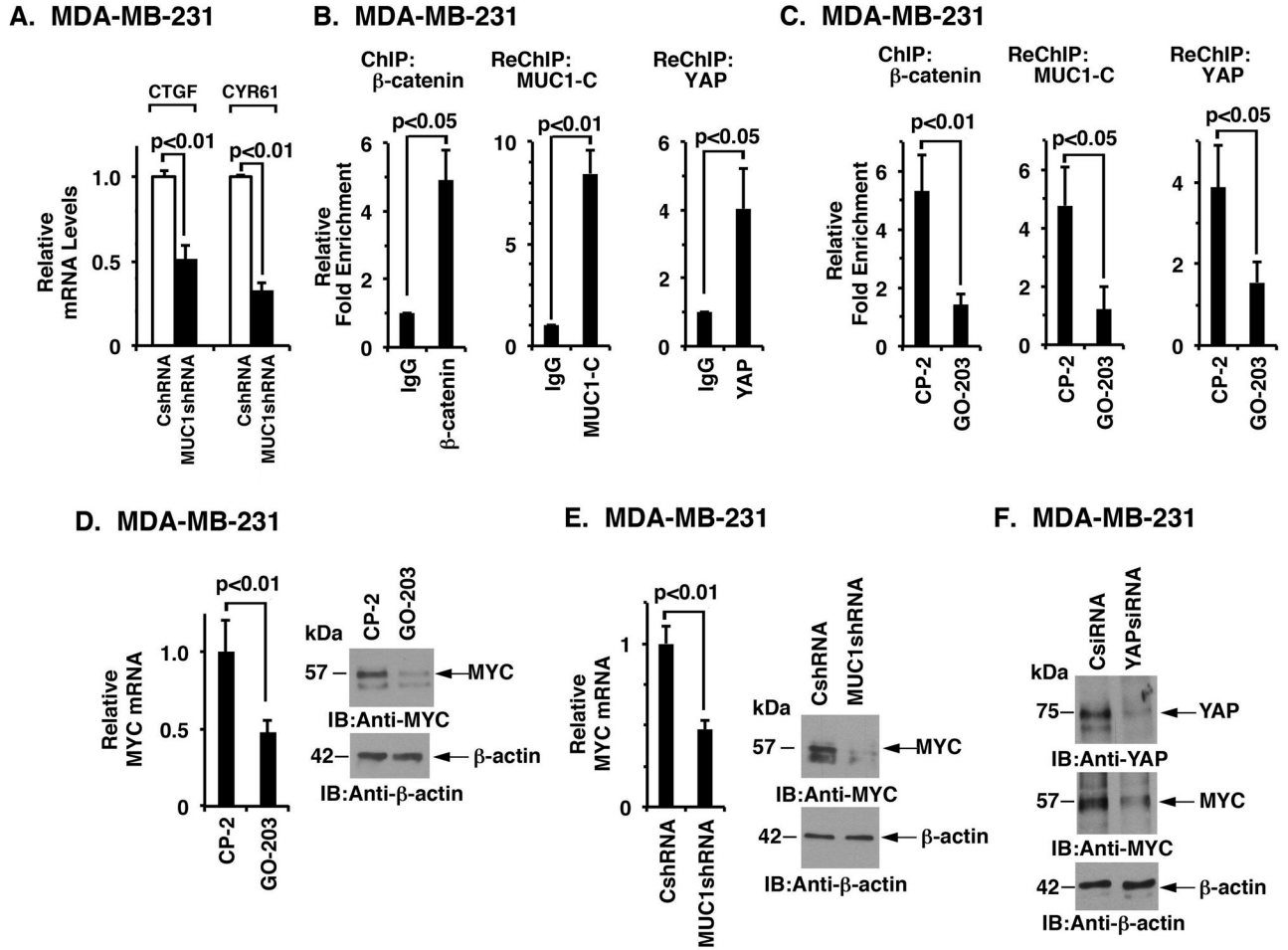


**Figure 6. MUC1-C associates with YAP and  $\beta$ -catenin on the *MYC* promoter**

A, The indicated MDA-MB-231 cells were analyzed for CTGF and CYR61 mRNA levels by qRT-PCR. The results are expressed as relative mRNA levels (mean $\pm$ SD of three determinations) as compared with that obtained for MDA-MB-231/CshRNA cells (assigned a value of 1). B, Soluble chromatin from the indicated MDA-MB-231 cells was precipitated with anti- $\beta$ -catenin or a control IgG (left). The final DNA precipitates were amplified by qPCR with pairs of primers for the  $\beta$ -catenin binding region in the *MYC* promoter region. Results are expressed as the relative fold enrichment (mean $\pm$ SD of three determinations) compared with that obtained for the IgG control (assigned a value of 1). For separate re-ChIP analysis, soluble chromatin from MDA-MB-231 cells was first precipitated with anti- $\beta$ -catenin, then released and reimmunoprecipitated with anti-MUC1-C (middle) or anti-YAP (right). The results (mean $\pm$ SD of three determinations) are expressed as the relative fold enrichment compared with that obtained with the IgG control (assigned a value of 1). C, MDA-MB-231 cells were treated with 5  $\mu$ M GO-203 or CP-2 each day for 3 days. Soluble chromatin was precipitated with anti- $\beta$ -catenin or a control IgG (left). For separate re-ChIP analysis, soluble chromatin from treated MDA-MB-231 cells was first precipitated with anti- $\beta$ -catenin, then released and reimmunoprecipitated with anti-MUC1-C (middle) or anti-YAP (right). The results (mean $\pm$ SD of three determinations) are expressed as the relative fold

enrichment compared with that obtained with the IgG control (assigned a value of 1). D, MDA-MB-231 cells treated with 5  $\mu$ M GO-203 or CP-2 each day for 3 days were analyzed for *MYC* mRNA by qRT-PCR (left). The results are expressed as relative *MYC* mRNA levels (mean $\pm$ SD of three determinations) as compared with that obtained for cells treated with CP2 peptide (assigned a value of 1). Lysates from MDA-MB-231 cells treated with 5  $\mu$ M GO-203 or CP-2 were immunoblotted with the indicated antibodies (right). E, MDA-MB-231 cells stably expressing a control scrambled shRNA (CshRNA) or a MUC1 shRNA were analyzed for *MYC* mRNA levels by qRT-PCR (left). The results are expressed as relative *MYC* mRNA levels (mean $\pm$ SD of three determinations) as compared with that obtained for MDA-MB-231/CshRNA cells (assigned a value of 1). Lysates from the MDA-MB-231/CshRNA and MDA-MB-231/MUC1shRNA cells were immunoblotted with the indicated antibodies (right). F, MDA-MB-231 cells were transiently transfected with a YAPsiRNA or a control siRNA (CsiRNA). Lysates were immunoblotted with the indicated antibodies.

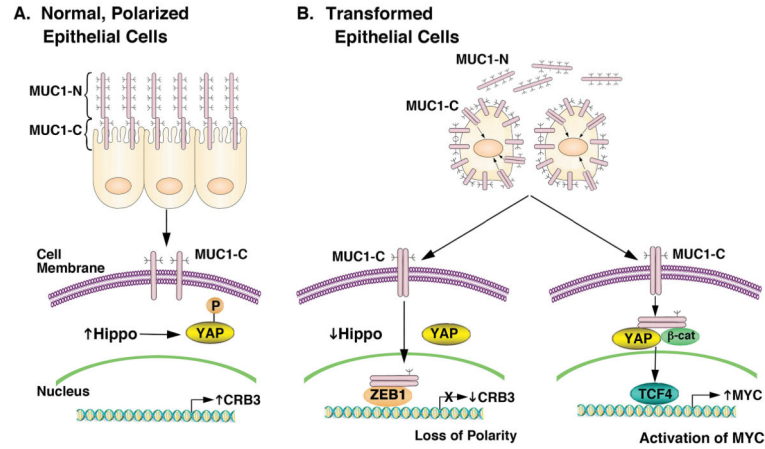


**Figure 7. Proposed schema depicting the role of MUC1-C in repression of *CRB3* expression, downregulation of the Hippo pathway and activation of YAP in TNBC cells**

A, The MUC1-N/MUC1-C complex is positioned at the apical borders of normal polarized epithelial cells (16, 17). MUC1-N protects the apical surface by forming a physical mucous barrier (16). The inactive MUC1-C subunit is poised to respond to stress signals, such as those induced by inflammation, toxins and microorganisms (16). Expression of *CRB3* is associated with maintaining polarity, activating the Hippo pathway and downregulating YAP by retention of p-YAP in the cytoplasm. B, With transformation and irreversible loss of polarity, MUC1 is upregulated at the cell membrane and MUC1-N is shed from the cell surface. In turn, MUC1-C forms homodimers that are transported into the nucleus by an importin- $\beta$ -mediated mechanism (16, 17). In the nucleus, MUC1-C forms a complex with ZEB1 on the *CRB3* promoter and represses *CRB3* transcription (left). Downregulation of *CRB3* expression is associated with suppression of the Hippo pathway and activation of YAP (left). Notably, MUC1-C/ZEB1 complexes also repress *miR-200c* expression with the induction of EMT (23). MUC1-C also binds directly to  $\beta$ -catenin, stabilizes  $\beta$ -catenin and promotes the formation of MUC1-C/YAP/ $\beta$ -catenin complexes in the nucleus, which associate with TCF4 and drive *MYC* expression (right). Based on this model and the present results, targeting MUC1-C with GO-203 in TNBC cells blocks MUC1-C homodimerization and thereby its nuclear import with upregulation of *CRB3* and activation of the Hippo tumor suppressor pathway.